# Apparent Faster-Than-Light Pulse Propagation in Interstellar Space: A new probe of the Interstellar Medium

F. A. Jenet[1], D. Fleckenstein[1], A. Ford [1], A. Garcia[1],R. Miller[1], J. Rivera[1], K. Stovall[1]

## ABSTRACT

Radio pulsars emit regular bursts of radio radiation that propagate through the interstellar medium (ISM), the tenuous gas and plasma between the stars. Previously known dispersive properties of the ISM cause low frequency pulses to be delayed in time with respect to high frequency ones. This effect can be explained by the presence of free electrons in the medium. The ISM also contains neutral hydrogen which has a well known resonance at 1420.4 MHz. Electro-magnetic theory predicts that at such a resonance, the induced dispersive effects will be drastically different from those of the free electrons. Pulses traveling through a cloud of neutral hydrogen should undergo "anomalous dispersion," which causes the group velocity of the medium to be larger than the speed of light in vacuum. This superluminal group velocity causes pulses containing frequencies near the resonance to arrive earlier in time with respect to other pulses. Hence, these pulses appear to travel faster than light. This phenomenon is caused by an interplay between the time scales present in the pulse and the time scales present in the medium. Although counter-intuitive, it does not violate the laws of special relativity. Here, we present Arecibo observations of the radio pulsar PSR B1937+21 that show clear evidence of anomalous dispersion. Though this effect is known in laboratory physics, this is the first time it has been directly observed in an astrophysical context, and it has the potential to be a useful tool for studying the properties of neutral hydrogen in the Galaxy.

*Subject headings:* pulsars: general — pulsars: individual (PSR B1937+21) — ISM: atoms — ISM: clouds

## 1. Introduction

A radio pulsar is a rapidly spinning neutron star that emits a beam of radio radiation. This highly columnated beam of radiation is rotated into and out of the line-of-sight of a distance observer as the star itself rotates about a fixed axis. Hence, an observer sees a periodic train of pulses arriving at regular intervals of time. The nature of these pulses gives astronomers a unique

[1]Center for Gravitational Wave Astronomy, University of Texas at Brownsville, TX 78520 (merlyn@phys.utb.edu)

tool to study various physical phenomena including electro-magnetic propagation effects in the interstellar medium (ISM).

Classically, pulsar pulses are affected by four basic ISM related propagation effects which can alter a pulse's observed properties: dispersion, absorption, Faraday rotation, and scattering (Manchester & Taylor 1977). Dispersion is caused by free electrons in the ISM (Cordes et al. 1991). Pulse absorption is caused by clouds of neutral hydrogen which absorb energy near the spin-flip resonance frequency of 1420.4 MHz (Weisberg et al. 2008; Johnston et al. 2001). The presence of a magnetic field together with free electrons cause Faraday rotation, which changes the orientation of the electric field's polarization vector (Han et al. 2006). Scattering effects are created by free electron density inhomogeneities (Armstrong et al. 1995). Recently, Weisberg et al. (2005) found evidence for stimulated emission driven by pulsar emission. Interstellar hydroxl (OH) clouds amplify the intensity of pulses with energy near the OH resonance. These four phenomena, together with the modern discovery of pulsar driven stimulated emission, encompass all previously known and studied ISM propagation effects.

This paper reports on the discovery of a new ISM propagation effect. The arrival times of pulses are seen to be delayed or advanced over and above the standard free-electron dispersion delay near the spin-flip resonance frequency of neutral hydrogen. In the next section, the physics of pulse dispersion is reviewed and the expected pulse time delay is calculated for the case of a cloud of neutral hydrogen with a thermal (i.e. Gaussian) velocity distribution. The observations and data analysis techniques used to measure this effected are presented in §3. The results and conclusions are given in §4.

## 2. Pulse dispersion in the ISM

The free electrons in the ISM induce a frequency dependent index of refraction, the ratio of the vacuum light propagation speed to the actual phase velocity in the medium. The index of refraction may be calculated directly from the "dispersion relationship", the equation which relates the wave number, $k$, to the wave's frequency, $f$. For the case of free electrons in the ISM, the dispersion relationship takes the following form assuming cgs units:

$$k = \frac{2\pi f}{c}\sqrt{1 - \frac{n_e e^2}{\pi m_e f^2}}, \tag{1}$$

where $n_e$ is the electron number density, $e$ is the electron charge, and $m_e$ is the electron mass. The index of refraction is given by $kc/2\pi f$, where c is the speed of light in vacuum. From the above dispersion relationship, one can calculate the index of refraction for free electrons:

$$n(f) = \sqrt{1 - \frac{n_e e^2}{\pi m_e f^2}}. \tag{2}$$

For frequencies greater than $\sqrt{n_e e^2/\pi m_e}$, the so called "plasma frequency", the index of refraction is less than unity. This implies that the phase velocity is greater than the speed of light. This is not a violation of any physical principal since it is well known that information propagates at the "group velocity," which is defined as the derivative of the angular frequency, $2\pi f$, with respect to the wavenumber, $k$. From equations 1 and 2, it can be shown that

$$v_{\rm group} = 2\pi df/dk = cn(f). \tag{3}$$

Since $n(f)$ is less than unity for frequencies above the plasma frequency, the group velocity is less than the speed of light in vacuum. The functional form of $n(f)$ tells us that high frequency pulses travel faster than low frequency pulses. Using the group velocity, one can calculate the time, $\Delta$, it takes for a pulse to travel from the pulsar to the telescope. Assuming that the free electron density is sufficiently low ($n_e << 10^7$ cm$^{-3}$ (f/1GHz)$^2$), which is true for observing frequencies above 22kHz, one can approximate $\Delta$ by its Taylor series expansion out to first order in $n_e$. One then finds that the propagation time may be written as a sum of two delays:

$$\Delta = \Delta_v + \Delta_{fe}, \tag{4}$$

where

$$\Delta_v = D/c, \tag{5}$$

$$\Delta_{fe}(f) = \frac{e^2 n_e D}{2\pi m_e c f^2}. \tag{6}$$

$D$ is the distance between the Earth and the pulsar, $\Delta_v$ is the vacuum propagation time, and $\Delta_{fe}(f)$ is the added frequency dependent delay due to the free electrons. Note that in order to simplify the discussion, it is assumed that the free electron density is uniform. The product $n_e D$ is known as the dispersion measure. If the free electron density varies along the line of sight, this product is replaced by the integral $\int_0^D n_e(l)dl$.

The presence of bound electrons can alter the index of refraction of a medium significantly near the resonance frequency (Jackson 1975; Sommerfeld 1954). $n(f)$ will have an imaginary part which is responsible for the absorption as well as a real part which determines the propagation properties. At resonance, the group velocity becomes greater than the speed of light in vacuum. This effect, a result of a phenomenon known as anomalous dispersion, can cause pulses to appear to travel faster-than-light without violating causality (Wang et al. 2000). Although the effects of anomalous dispersion have been measured in ground based laboratories (Schweinsberg et al. 2006; Dogariu et al. 2001), they have not been observed in an astrophysical context. Pulsar observations offer a unique opportunity to directly measure the effects of anomalous dispersion using the electron spin-flip transition in neutral hydrogen.

Consider the case of a medium made up of a cloud of neutral hydrogen only. First, lets assume that the atoms are not moving with respect to the observer. In this case, the dispersion relationship

takes the form (Jackson 1975):

$$k^2c^2 = (2\pi f)^2 - \frac{\left(n_h e^2 s_h/\pi m_e\right)(2\pi f)^2}{f^2 - f_0^2 + i2\frac{f}{\tau}} \tag{7}$$

where $n_h$ is the number density of hydrogen, $s_h$ is the "oscillator strength," $\tau$ is the life time of the spin-flip transition, and $f_0$ is the resonant frequency of the transition. Note that $n_h$ is the number density only when the spin temperature is zero. Otherwise, its the difference between the number density of atoms with its electron spin in its ground state minus the number density of atoms with its electron spin in its excited state. From the above dispersion relationship, the squared index of refraction is given by

$$n(f)^2 = 1 - \frac{\left(n_h e^2 s_h/\pi m_e\right)}{f^2 - f_0^2 + i2\frac{f}{\tau}} \tag{8}$$

It will be assumed that we are only interested in frequencies near $f_0$. Since $f_0 = 1.4$ GHz and the observing bandwidth is of order 1 MHz, $|f - f_0|/f_0 << 1$. In this case, one can approximate $f^2 - f_0^2$ as $2f(f - f_0)$. With this approximation, the squared index of refraction becomes:

$$n(f)^2 = 1 - \frac{\left(n_h e^2 s_h/2\pi m_e f\right)}{f - f_0 + i\frac{1}{\tau}} \tag{9}$$

If the atoms were moving with respect to the observer at speeds small compared to the speed of light, $f_0$ in the denominator of the above expression would be replaced by its Doppler-shifted value of $f_0(1 - v/c)$ where $v$ is the radial velocity. If one were to add in another set of atoms moving at a velocity different from the first set, the index of refraction would be adjusted simply by adding another term of a form identical to the second term in the above expression except with different values of $n_h$ and $f_0$. Following this logic, the squared index of refraction for the case of a cloud of neutral hydrogen with a thermally distributed set of radial velocities takes the form:

$$n(f)^2 = 1 - \frac{n_h e^2 s_h}{2\pi m_e f}\frac{1}{\sqrt{2\pi} f_d}\int \frac{e^{\frac{-(f'-f_c)^2}{2f_d^2}}}{f - f' + i\frac{1}{\tau}} df', \tag{10}$$

where $f_c = f_0(1 - v_c/c)$, $v_c$ is the average velocity of the cloud, $f_d = f_0\sqrt{k_b T/m_h c^2}$ is the thermal frequency width of the cloud, $k_b$ is Boltzmann's constant and $T$ is the kinetic temperature of the cloud.

The integral on the right hand side of equation 10 may be evaluated analytically in terms of the $w(z)$ function defined in Abramowitz & Stegun (1970), section 7. In terms of $w(z)$, the squared index of refraction becomes:

$$n(f)^2 = 1 + \frac{i n_h e^2 s_h}{2\sqrt{2\pi} m_e f f_d} w\left(\frac{f - f_c + i/\tau}{\sqrt{2} f_d}\right) \tag{11}$$

Since $w(z) \leq 1$ provided that the imaginary part of $z$ is greater than zero, the maximum amplitude of the second term in equation 11 is given by $n_h e^2 s_h/2\sqrt{2\pi} m_e f_d^2$. A full quantum mechanical

treatment shows that $s_h = hf_0/2mc^2$ where h is Planck's constant (Condon & Shortley 1963). Hence, the maximum amplitude is much less than unity as long as $n_h << 10^{21}\mathrm{cm}^{-3}$. Under this assumption, we can accurately approximate $n(f)$ by:

$$n(f) = 1 + \frac{in_h e^2 s_h}{4\sqrt{2\pi} m_e f f_d} w\left(\frac{f - f_c + i/\tau}{\sqrt{2} f_d}\right) \tag{12}$$

In order to simplify further the above expression, we will ignore the natural line width term, $i/\tau$, since it is much less than the Doppler broadening width $f_d$. Also, we will define $\sigma_o = \sqrt{\pi} n_h e^2 s_h / \sqrt{2} m_e f_d c$. The index of refraction may now be written as:

$$n(f) = 1 + \frac{i\sigma_0 c}{4\pi f} w\left(\frac{f - f_c}{\sqrt{2} f_d}\right) \tag{13}$$

There were several approximations used to derived the above expression for the index of refraction. These approximations are summarized here. First, it is necessary that $1/\tau << f_d << f_0$. Since $f_d$ is determined by the cloud temperature, it can be shown that the above expression for $n(f)$ is valid as long as $10^{-26}\mathrm{K} << T << 10^{14}\mathrm{K}$. Second, the number density of hydrogen atoms in the cloud must be less than $10^{21}\mathrm{cm}^{-3}$. Both of these conditions are easily satisfied in the ISM where the cloud temperatures range from 10 K up to $10^4$ K and the densities range from less than $0.01\mathrm{cm}^{-3}$ to of order $100\mathrm{cm}^{-3}$ (Burke & Graham-Smith 2002). Note, there is evidence of HI clouds with densities up to $10^4\mathrm{cm}^3$ (Johnston et al. 2003), but even this relatively high density is still well within the regime of validity for equation 13.

The index of refraction determines both the rate at which the intensity of the wave-packet decreases as well as the time it takes for the wave-packet to travel through the medium. The intensity of the wave-packet decreases as $e^{-\sigma(f)D}$ where $\sigma(f)$ is the frequency dependant absorption coefficient and $D$ is the distance traveled through the cloud. The absorption coefficient is determined from the imaginary part of the index of refraction: $\sigma(f) = \mathrm{Im}(4\pi f n(f)/c)$. From equation 13, one finds that $\sigma(f)$ is proportional to the real part of $w(z)$, which is identically equal to $e^{-z^2}$ when $z$ is purely real (See Abramowitz & Stegun (1970), section 7.1). Given $\sigma(f)$ and the length scale of the cloud, $D_c$, the optical depth of the cloud, $\tau$, may be calculated:

$$\tau(f) = \sigma(f) D_c = \tau_0 e^{-\frac{(f-f_c)^2}{f_d^2}}, \tag{14}$$

where $\tau_0 = \sigma_0 D_c$.

The real part of $n(f)$ determines the propagation properties of the wave. The propagation time across a cloud is determined by $\Delta(f) = D_c / v_{\mathrm{group}}(f) = (D_c/c)\mathrm{Re}[dk/df]/2\pi = (D_c/c) d(fn(f))/df$. For the index of refraction given in equation 13, $\Delta(f)$ may be written as

$$\Delta(f) = \frac{D_c}{c} + \frac{\sigma_0 D_c}{4\sqrt{2}\pi f_d} \mathrm{Re}\left[iw'\left(\frac{f - f_c}{\sqrt{2} f_d}\right)\right] \tag{15}$$

where $w'(z) = dw(z)/dz$. As for the case of the free electrons, one can see that the propagation time may be written as a sum of the vacuum delay term and a term involving the hydrogen resonance: $\Delta(f) = D_c/c + \Delta_{rd}(f)$. Abramowitz & Stegun (1970) gives an expression for $w'(z)$ in terms of $w(z)$: $w'(z) = -2zw(z) + 2i/\sqrt{\pi}$. Using this, the resonant dispersion component of the time delay, $\Delta_{rd}(f)$, may be written as:

$$\Delta_{rd}(f) = \tau_0 \left( \frac{f - f_c}{4\pi f_d^2} \right) \mathrm{Im} \left[ w \left( \frac{f - f_c}{f_d} \right) \right] - \frac{\tau_0}{2\sqrt{2}\pi^{3/2} f_d}. \tag{16}$$

As an example of what we might expect see in actual data, Figure 1 shows the absorption spectrum given by $e^{-\tau(f)}$ and the frequency dependent delay, $\Delta_{rd}(f)$, for a single hydrogen cloud. The peak optical depth is unity and the temperature is $100K$. Near the peak of the resonance, $\Delta_{rd}(f)$ is less than zero, implying that the pulses arrive earlier in time.

The unique shape of the frequency dependent delay warrants further discussion. The time delay is proportional to $1/v_{group} = n(f) + f dn(f)/df$. For most frequencies, the dispersion is 'normal' where normal dispersion is defined as $dn(f)/df > 0$. Within a small range of frequencies near resonance, $dn(f)/df < 0$ and the dispersion is said to be 'anomalous'. If the magnitude of $dn(f)/df$ is sufficiently large, as is the case for HI resonant dispersion, the delay will become negative. Since the dispersion is normal for most frequencies and since $dn(f)/df$ is continuous, there must be regions on either side of the anomalous dispersion region where the dispersion transitions back to normal. It just so happens that the transition regions are still close enough to resonance so that normal dispersion is enhanced thus producing the delay 'wings' to either side of the anomalous dispersion negative delay peak. Further discussion of this phenomenon may be found in Jackson (1975), section 7.8.

The reason that this pulse advance is not a violation of causality and relativity is a subtle one. Put simply, the peak of the pulse does not necessarily carry information. When the rising edge of the pulse enters the plasma, it causes the atoms to start emitting radiation at the same frequencies as that present in the wave-packet, but each with a slightly different phase. This radiation interferes with the radiation in the wave-packet in just the right way as to cause the intensity to start to decrease earlier than it would have in vacuum. Hence, the peak has advanced. It will not advance earlier than the time the leading edge reached the plasma.

Lets assume that we wanted to create a signal transmission device that could send information faster than the speed of light using the anomalous dispersion effect. We could imagine having a pulse generator that, when a button is pressed, emits a wave packet with frequency content near the HI resonance into an HI cloud. The pulse would travel through the cloud and hit a receiver at some distance $D$ away. For argument sake, lets assume that the pulse envelope is described by a Gaussian function with a given width. The device is setup so that, initially, it is not transmitting. As soon as the button is pressed, the device starts to transmit the signal. If we let $E(x,t)$ represent the electric field of the signal and say that the button is pressed at $t = 0$, then $E(0,t) = 0$ for all times less than zero and it is non-zero at $t > 0$. It can be shown formally that $E(D,t)$ must

be equal to zero for all times $t < D/c$ (Jackson 1975). The transmission device was programed to emit a pulse whose peak power occurs at some known duration after the button is pressed. No matter what happens to the peak of the pulse, it cannot arrive earlier than $D/c$. The peak will have occured at some positive time after the button is pressed. As it travels through the HI cloud, the peak may be moving faster than light for some distance, but it will still arrive after a time $D/c$, the earliest time when information about the button being pressed could be received. It may be the case that the receiver detects the signal only after a threshold intensity is reached. In which case, the signal traveling through the HI cloud may be detected before the signal traveling through vacuum, but the detection will occur after a time $D/c$. Note that if the peak continued to move at a rate fater than light, the peak would eventually arrive earlier than $D/c$. In this extreme case, the assumptions used to calculate the group velocity break down and the group velocity no longer describes the propagation of the peak. As long at the time shift is small compared to the width of the pulse, the group velocity will describe the propagation of the peak of the pulse and the pulse shape itself will not change (Garrett & McCumber 1970).

In the ISM, there can be free electrons present together with neutral hydrogen. In this case, the total time delay is a sum of the free electron delay together with the time delays associated with each HI cloud present along the line-of-sight to the pulsar. It should be emphasized that the anomalous dispersion effects are completely separate from the normal dispersion effects of the free electrons. One may be tempted to side-step the whole causality issue discussed above by saying that the pulses are advanced by a small amount with respect to a much larger pulse delay introduced by the free electrons. If the free electrons and the neutral hydrogen were somehow always forced to occupy the same regions of space, this may be a valid argument. The fact of the matter is that the neutral hydrogen may very well be located in regions of space distinct from the free electrons. Pulses traveling through the HI regions will appear to travel faster than light.

## 3. Observations and Analysis

Previous pulsar pulse arrival time observations have all been consistent with free electron dispersion. Observations presented here show the presence of anomalous dispersion at the resonance frequency of the hydrogen spin-flip transition. Using the Arecibo[1] 305m radio telescope, pulsar PSR B1937+21 was observed using the L-Band wide receiver centered on 1420.4 MHz. The data were recorded using the Wide-band Arecibo Pulsar Processor (WAPP) using 128 frequency channels across a 1.5 MHz bandwidth. Both polarizations were summed together. Data were taken over three days. Observations lasted for 2 hours during the first observing session, and 1.5 hours on the other days. For each day, average pulse profiles were obtained in each channel using this source's known phase parameters (i.e. its ephemeris). From the folded profiles in each frequency channel, a pulse arrival time was obtained by convolving the measured profile with an analytic

[1]The Arecibo Observatory is operated by Cornell University under contract from the National Science Foundation

profile consisting of two Gaussian pulses. The parameters of the analytic profile were obtained by fitting the measured pulsar profile. The effects of dispersion were removed using standard incoherent dedispersion techniques (Lorimer & Kramer 2004). Hence, the analytic profile was a good representation of the average profile but without the added receiver noise. See Lorimer & Kramer (2004) for details of pulsar timing techniques.

Figure 2 shows the measured pulse times-of-arrival relative to the lowest frequency channel as a function of frequency. The three panels correspond to the three different observing days. Over the 1.5 MHz band, the free electron dispersion delay, $\Delta_{df}$, can be well approximated by a linear function of the frequency offset from the center of the band. This linear trend was subtracted from the delays presented in figure 2. The expected pulse advances are clearly seen in all three days. The reproducible features are caused by the structure and velocity of the hydrogen clouds located between Earth and the pulsar.

Figure 3 shows the measured anomalous dispersion delays averaged over all three observing runs together with the hydrogen emission and absorption spectra measured from the same data. Note that these emission and absorption spectra are consistent with previously published results by Heiles et al. (1983). From the figure, it can been seen that the structure in the anomalous dispersion "delay spectrum" is consistent with the features seen in absorption. Note that digitization effects are known to alter the absorption spectrum (Weisberg et al. 1980). Such systematic effects have been removed from the absorption spectrum.

It is possible that digitization effects could be affecting the delay spectrum. In order to determine if digitization could be causing or altering the measured delay spectrum, Monte-Carlo style simulations were performed. Several million simulated pulses were generated by modulating Gaussian noise with a Gaussian pulse profile. The effects of the free electron and neutral hydrogen dispersion were added to the signal by Fourier transforming the data into the frequency domain using the Fast Fourier Transform technique (FFT), multiplying the transformed data by a filter function derived from the appropriate dispersion relationship, and then transforming the data back into the time domain. The pulsar had a simulated period and dispersion measure equal to that of PSR B1937+21. The simulated signal had a 1.5 MHz bandwidth. The HI cloud was given a temperature of 100 K and a peak optical depth of 1.6. Random Gaussian deviates were then added to the data to simulate the effects of receiver noise. The noise level was chosen to be consistent with the L-band wide receiver system. These data were next digitized into n-bits and then broken up into 128 independent frequency channels using an FFT based technique. The signal in each channel was then squared and folded at the pulsar period. This resulted in a folded filterbank in the same form as the actual data taken with the WAPPs. Delay spectrum plots were then made in exactly the same way as done using the real data. A delay spectrum was made using 2-bits and compared to one made with 32-bits. No significant differences were seen in the data sets. As an extreme test, the real part of the HI cloud's index of refraction was set to zero, thus removing the anomalous dispersion pulse arrival time delays/advances. This test would determine if the digitization process was somehow artificially causing systematic arrival time delays/advances because of the frequency

dependant absorption. No significant features were seen in this delay spectrum. The above tests were also done with no receiver noise added to the data. Again, no significant features were seen in the delay spectrum. Hence, it was concluded that digitization does not introduce significant artifacts into the delay spectrum.

## 4. Results and Conclusions

The delay spectrum offers a completely new way to probe neutral hydrogen clouds. The information obtained can be used together with the absorption information to create a more accurate understanding of a cloud's properties. It should be noted that the delay spectrum carries different information than the absorption spectrum. The peak of the absorption spectrum scales as the absorption parameter, $\tau_0$, which is proportional to the HI column density divided by $f_d$ (See equation 13 and the definition of $\sigma_0$ above it. Remember that $\tau_0 = \sigma_0 D_c$ and the column density is given by $n_h D_c$). Since $f_d$ is proportional to $T^{1/2}$, $\tau_0$ scales as $T^{-1/2}$ times the HI column density. The peak of the delay spectrum, given by

$$\Delta_{peak} = -\frac{\tau_0}{(2\pi)^{3/2} f_d}, \tag{17}$$

scales as $\tau_0/f_d$. Hence, the peak delay scales as the HI column density times $T^{-1}$. This difference in the temperature dependence will break the degeneracy between the kinetic temperature and the column density that exists with only the absorption information alone. The data presented here illustrates this idea.

The absorption spectrum in 3 contains both broad and narrow-line features. There appears to be about four narrow line features whose peaks line up with the peaks seen in the delay spectrum. Taking the full-width-half-maximum (FWHM) of these features to be of order two bins (23 kHz), which corresponds to a kinetic temperature of about 500 K, the expected delay given by equation 17 is of order 10 microseconds. This is consistent with the observed delay spectrum. Note that the two largest peaks in the delay spectrum have the largest errors since the absorption is the greatest at this point. If the delay is actually at 25 microseconds, as suggest by the data, then there would have to exist narrow-band, $\approx$ 10 kHz, unresolved clouds at these locations. The necessary kinetic temperatures would have to be about 100 K.

There are also two broad features seen in the data, the first centered at about 1420.3 MHz, and the other starts just above 1420.4 MHz. It is not possible to determine the kinetic temperatures of the clouds in these regions from the absorption spectrum alone since one cannot measure a line-width. One can use equation 17 together with the delay spectrum to estimate the cloud bandwidths and kinetic temperatures. For the region centered at 1420.3 MHz, the measured optical depth is .4 and the delay is .9 microseconds. If this region were made up of a set of clouds with kinetic temperatures of the same order as the narrow-line features (i.e. 500 K), but with smaller optical depths,the measured delays would have to be of order 2.5 microseconds, a factor of over 2.5 times the measured value. Using equation 17 together with the measured optical depth and delay, the

kinetic temperature of a single cloud in this region would have to be 5000 K. The FWHM of such a cloud is 70 kHz. Hence, a single hot cloud could explain the data in this region. Considering the region above 1420.4 MHz, the optical depth in this region is around .2 while the delay is about 3 microseconds. This corresponds to a cloud temperature of about 100 K and FWHM of 10 kHz. This width is just under the frequency resolution of the data. Hence, a single high temperature cloud in this region cannot explain the data. It must be made up of about 5 unresolved clouds each with temperatures of about 100 K. It should be noted that this is consistent with high spectral resolution observations of other pulsars that have revealed the existence of absorption features as narrow as 2 kHz (Johnston et al. 2003; Stanimirović et al. 2003; Frail et al. 1994).

Given the signal-to-noise ratio and frequency resolution of the current data, it is difficult to make any definitive statements about the underlying cloud structure aside from the estimates made above. Also, the analysis presented here assumes distinct HI clouds in local thermodynamic equilibrium so that the atomic velocity distribution is given by a Gaussian distribution and the temperature refers to the thermal velocity width along the line of sight. Future observations with longer time integrations and higher frequency resolution together with more sophisticated analysis techniques that take into account more complicated, perhaps turbulent, velocity distributions should enable us to determine or at least place bounds on the number, average temperature, and column density of the neutral hydrogen clouds in the line of sight to this pulsar. These techniques can also be applied to a larger set of pulsars. This will allow us to gain further insight into the global structure of neutral hydrogen in the Milky-Way.

The lead author wants to thank J. Dawson for discussions which inspired this work, M. Nolan for his help in obtaining the time at Arecibo, Phil Perillat and Arun Venkataraman for their invaluable assistance in setting up the observations, R. Braun, S. Johnston, B. Koribalski, B. Rickett, D. Stinebring, and J. Weisberg for their insights and encouragement during the preparation of this manuscript. The observations were preformed by students involved in the Arecibo Remote Command Center (ARCC), a program designed to involve students in research early in their career. This work was supported by a CAREER grant from the National Science Foundation (award AST 0545837).

## REFERENCES

Abramowitz, M., & Stegun, I. A. 1970, Handbook of mathematical functions : with formulas, graphs, and mathematical tables

Armstrong, J. W., Rickett, B. J., & Spangler, S. R. 1995, ApJ, 443, 209

Burke, B. F., & Graham-Smith, F. 2002, An Introduction to Radio Astronomy: Second Edition

Condon, E. U., & Shortley, G. H. 1963, The theory of atomic spectra

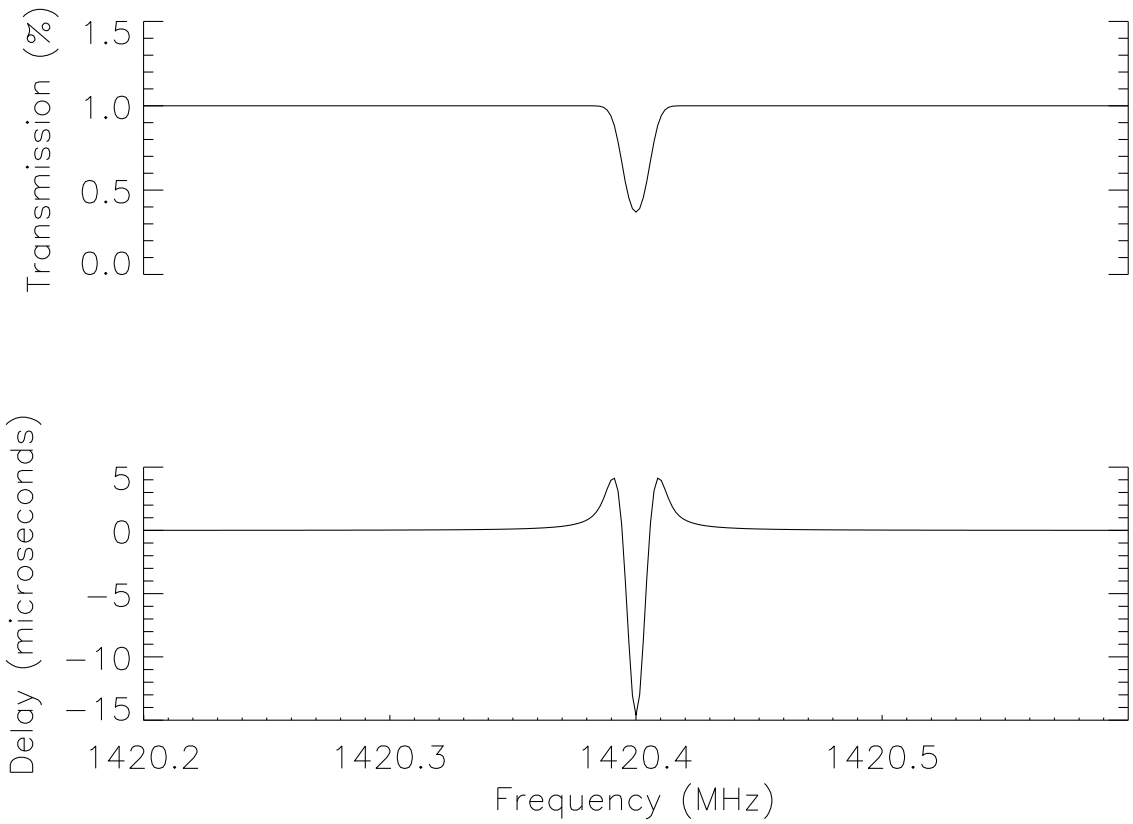


Fig. 1.— The expected absorption (top) and delay (bottom) spectrum caused by a cloud of neutral hydrogen (HI) in the ISM. The kinetic temperature is 100K and the optical depth is unity. At the spin-flip transition frequency, the delay is seen to be negative, corresponding to a pulse advance. Pulses at this frequency appear to arrive earlier then pulses at frequencies off resonance. Note, the free electron dispersive effects are not included in the above delay spectrum.

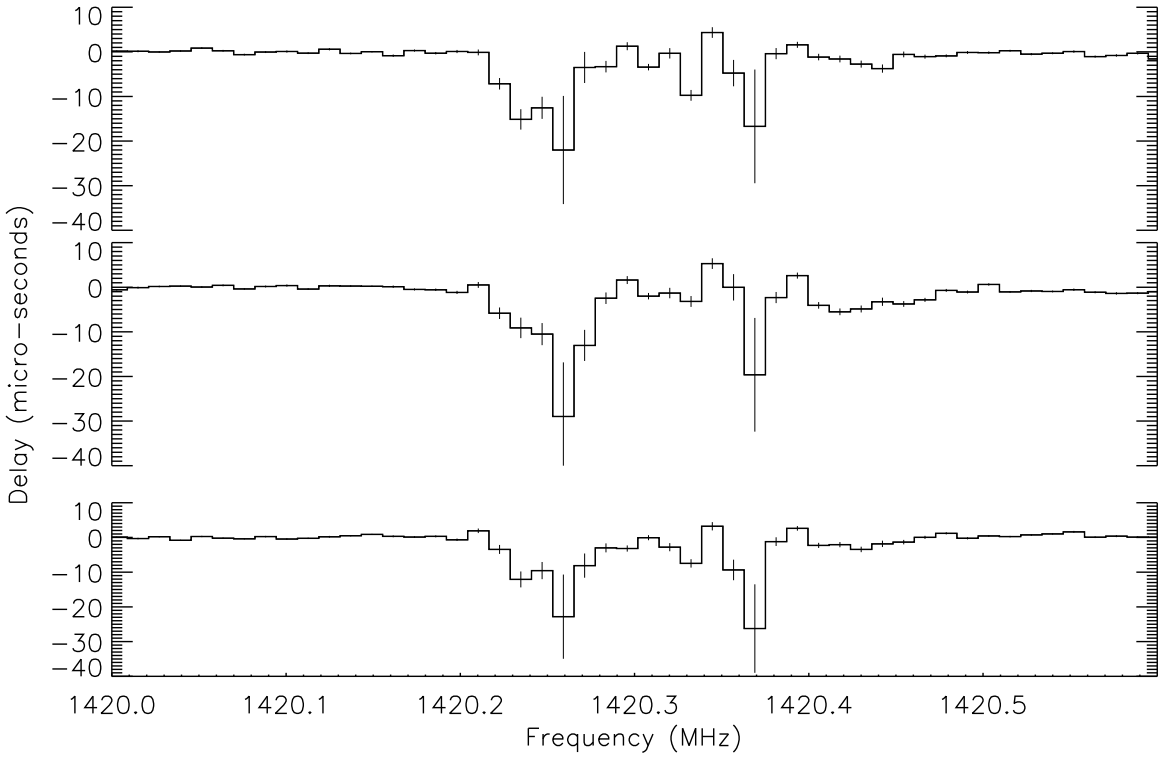


Fig. 2.— The delay spectra measured on three consecutive days. The top panel, day 1, was measured using a two hour observation. The remaining two days correspond to 1.5 hour observations.

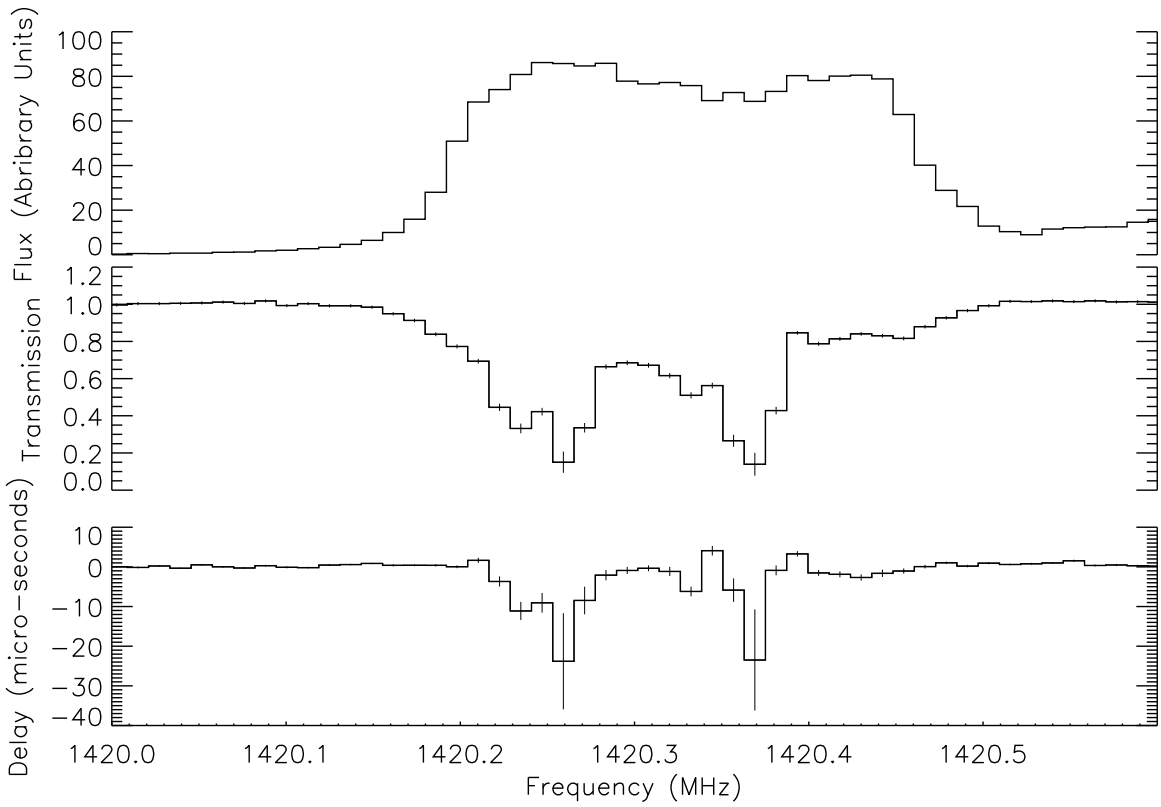


Fig. 3.— The measured neutral hydrogen emission spectrum (top), absorption spectrum (middle), and delay spectrum (bottom). The free electron dispersive effects were removed from the data by subtracting the best fit linear model to the delay data using the off-resonance frequencies. The $1-\sigma$ error bars take into account the increased system temperature due to the line emission as well as the reduced signal due to the absorption spectrum.

Cordes, J. M., Weisberg, J. M., Frail, D. A., Spangler, S. R., & Ryan, M. 1991, Nature, 354, 121

Dogariu, A., Kuzmich, A., & Wang, L. J. 2001, Phys. Rev. A, 63, 053806

Frail, D. A., Weisberg, J. M., Cordes, J. M., & Mathers, C. 1994, ApJ, 436, 144

Garrett, C. G., & McCumber, D. E. 1970, Phys. Rev. A, 1, 305

Han, J. L., Manchester, R. N., Lyne, A. G., Qiao, G. J., & van Straten, W. 2006, ApJ, 642, 868

Heiles, C., Kulkarni, S. R., Stevens, M. A., Backer, D. C., Davis, M. M., & Goss, W. M. 1983, ApJ, 273, L75

Jackson, J. D. 1975, Classical electrodynamics

Johnston, S., Koribalski, B., Weisberg, J. M., & Wilson, W. 2001, MNRAS, 322, 715

Johnston, S., Koribalski, B., Wilson, W., & Walker, M. 2003, MNRAS, 341, 941

Lorimer, D. R., & Kramer, M. 2004, Handbook of Pulsar Astronomy

Manchester, R. N., & Taylor, J. H. 1977, Pulsars.

Schweinsberg, A., Lepeshkin, N. N., Bigelow, M. S., Boyd, R. W., & Jarabo, S. 2006, Europhysics Letters, 73, 218

Sommerfeld, A. 1954, Optics Lectures on Theortical Physics, Vol. IV

Stanimirović, S., Weisberg, J. M., Hedden, A., Devine, K. E., & Green, J. T. 2003, ApJ, 598, L23

Wang, L. J., Kuzmich, A., & Dogariu, A. 2000, Nature, 406, 277

Weisberg, J. M., Johnston, S., Koribalski, B., & Stanimirović, S. 2005, Science, 309, 106

Weisberg, J. M., Rankin, J., & Boriakoff, V. 1980, A&A, 88, 84

Weisberg, J. M., Stanimirović, S., Xilouris, K., Hedden, A., de la Fuente, A., Anderson, S. B., & Jenet, F. A. 2008, ApJ, 674, 286